

Figure 1. Isolation and characterization of phage-resistant mutants of BMB171 and regained-infectivity phage mutants of vB_BthS_BMBphi. (A) Phage-resistant mutants of BMB171 isolated in this study. (B) Infectivity of regained-infectivity phage mutants vB_BthS_BMBphi-M1 to the phage-resistant strains and BMB171. (C) The mobility of the strains BMB171 and the phage-resistant mutants. The agar plate with a concentration of 0.3% was used for bacterial mobility analysis. (D) Comparison of the bacterial clone size of strain BMB171 and the phage-resistant mutants. For each strain, 30 clones were used for the analysis of the clone diameters, and the asterisk indicates a significant difference ($p < 0.05$) between the diameter of different bacterial clones.

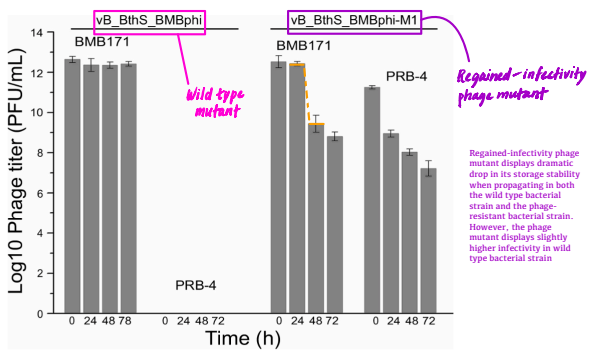
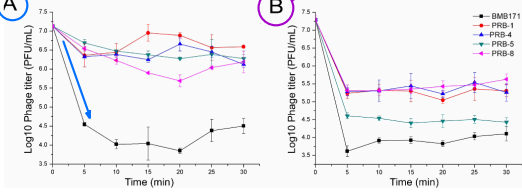


Figure 2. Storage stability of the phage vB_BthS_BMBphi and vB_BthS_BMBphi-M1. The infectivity of the two phages was tested against the strains BMB171 and PRB-4, respectively, after storage for 24, 48, and 72 h.

Binding Affinity Assay

Phage titre was measured every 5 minutes during the adsorption stage. T1 wild type phage vB_BthS_BMBphi or displays binding affinity to the wild type bacterial host.



The regained-infectivity phage mutant exhibits binding affinity to all other first generation phage-resistant mutants.

Figure 3. Adsorption of phage vB_BthS_BMBphi (A) and vB_BthS_BMBphi-M1 (B) to strain BMB171 and four phage-resistant mutants.

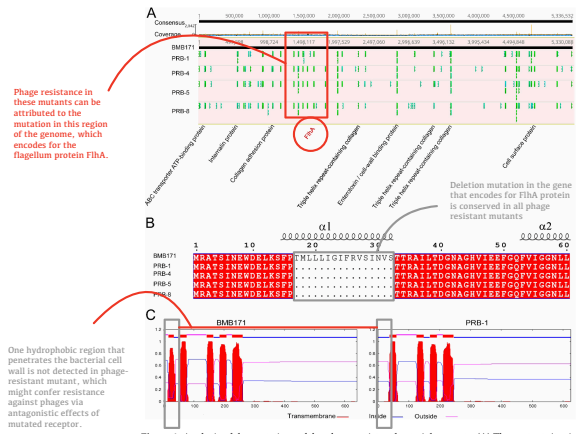


Figure 4. Analysis of the mutations of the phage-resistant bacterial mutants. (A) The mutant sites in four phage-resistant bacterial mutants. The functions and locations of the cell surface proteins that mutated in all the four mutants are indicated. (B) Alignment of the protein FliA from the strains BMB171 and four phage-resistant mutants. The secondary structures of the protein are indicated. (C) Transmembrane domain of protein FliA from strain BMB171 and PRB-1.

